

**International Journal of Machining and Machinability of Materials**

ISSN online: 1748-572X - ISSN print: 1748-5711

<https://www.inderscience.com/ijmmm>

---

**3D FE cutting simulations of Nomex honeycomb composites in rotary ultrasonic machining process**

Shahzad Ahmad, Jianfu Zhang, Jianjian Wang, Pingfa Feng, Xiangyu Zhang

**DOI:** [10.1504/IJMMM.2024.10061017](https://doi.org/10.1504/IJMMM.2024.10061017)

**Article History:**

Received:	26 February 2023
Last revised:	17 June 2023
Accepted:	29 June 2023
Published online:	18 March 2024

---

## **3D FE cutting simulations of Nomex honeycomb composites in rotary ultrasonic machining process**

---

**Shahzad Ahmad**

Beijing Key Laboratory of Precision/  
Ultra-Precision Manufacturing Equipment and Control,  
Department of Mechanical Engineering,  
Tsinghua University,  
Beijing, 100084, China  
and  
Department of Mechanical Engineering,  
Muhammad Nawaz Sharif University of Engineering and  
Technology (MNS UET),  
Multan 60600, Pakistan  
Email: drshahzad.tsinghua@gmail.com

**Jianfu Zhang\***

Beijing Key Laboratory of Precision/  
Ultra-Precision Manufacturing Equipment and Control,  
Department of Mechanical Engineering,  
Tsinghua University,  
Beijing, 100084, China  
and  
State Key Laboratory of Tribology,  
Department of Mechanical Engineering,  
Tsinghua University,  
Beijing, 100084, China  
Email: zhjf@tsinghua.edu.cn  
\*Corresponding author

**Jianjian Wang**

Beijing Key Laboratory of Precision/  
Ultra-Precision Manufacturing Equipment and Control,  
Department of Mechanical Engineering,  
Tsinghua University,  
Beijing, 100084, China  
Email: wangjjthu@tsinghua.edu.cn

## Pingfa Feng

Beijing Key Laboratory of Precision/  
Ultra-Precision Manufacturing Equipment and Control,  
Department of Mechanical Engineering,  
Tsinghua University,  
Beijing, 100084, China  
and  
State Key Laboratory of Tribology,  
Department of Mechanical Engineering,  
Tsinghua University,  
Beijing, 100084, China  
Email: fengpf@mail.tsinghua.edu.cn

## Xiangyu Zhang

Beijing Key Laboratory of Precision/  
Ultra-Precision Manufacturing Equipment and Control,  
Department of Mechanical Engineering,  
Tsinghua University,  
Beijing, 100084, China  
Email: aquilani@tsinghua.edu.cn

**Abstract:** In this research a 3D FE rotary ultrasonic cutting simulation model of NHCs core material was developed based on Hashin failure criterion and novel ultrasonic circular saw blade cutter system. Further, 3D FE cutting simulation model was validated by performing RUM experiments on ultrasonic machine tool and explored. Cutting force exhibits inverse relation with vibration amplitude and spindle speed of ultrasonic circular saw blade tool, whereas it shows direct relation with feed rate. Finally, an optimised set of processing parameters was obtained by performing series of cutting simulations and verified by experimental work with a novel ultrasonic circular saw blade cutting tool at resonant frequency of 22,050 Hz, spindle speed 3,000 rpm, feed rate 500 mm/min, cutting width 8 mm, cutting depth 2 mm, and vibration amplitude 25  $\mu\text{m}$ . Moreover, this study provides systematic guideline for RUM process optimisation and improvements of surface quality.

**Keywords:** 3D FE modelling; cutting simulations; Nomex honeycomb composites; NHCs; rotary ultrasonic machining; RUM; processing parameters optimisation; chips formation.

**Reference** to this paper should be made as follows: Ahmad, S., Zhang, J., Wang, J., Feng, P. and Zhang, X. (2024) '3D FE cutting simulations of Nomex honeycomb composites in rotary ultrasonic machining process', *Int. J. Machining and Machinability of Materials*, Vol. 26, No. 1, pp.58–84.

**Biographical notes:** Shahzad Ahmad has received his PhD in Mechanical Engineering from Tsinghua University Beijing China in January 2022. His research interests mainly include but not limited to the development of ultrasonic machining systems, customised ultrasonic cutting tools, non-conventional processing of various advanced aerospace materials like composites (aramid fibre, CFRPs, GFRPs), titanium alloys (Ti-6Al-4V), finite

element and multi-physics simulations, additive manufacturing, materials characterisations analysis and NDT testing. He has registered a patent, published various papers and presented research in international conferences.

Jianfu Zhang is an Associate Professor (tenured) and PhD Supervisor in the Department of Mechanical Engineering, Tsinghua University Beijing, China. His research interests include damage formation mechanism and control methods in rotary ultrasonic drilling, ultrasonic micro-nano manufacturing technology, design theory, method of giant magnetostrictive ultrasonic machining system; intelligent manufacturing and digital twin technology. As PI, he has completed more than 30 national, provincial and industrial projects. He has published more than 160 research papers, applied 86 patents (50 of them were authorised), achieved 28 software copyrights, and received national and provincial level scientific and technology awards 11 times.

Jianjian Wang is an Assistant Professor in the Department of Mechanical Engineering, Tsinghua University Beijing China. His research interests mainly include high-performance ultrasonic vibration assisted machining process and equipment, micro/nano machining of bio-inspired functional structures, design and application of acoustic metamaterials. He has received various awards national and international level such as Alexander von Humboldt Research Fellowship, 2019, excellent PhD Thesis at Tsinghua University, 2018, and excellent Master Thesis at Tsinghua University, 2014. He has published various papers and presented research in international conferences.

Pingfa Feng is a Professor and PhD Supervisor in the Department of Mechanical Engineering, Tsinghua University Beijing, China. His research interests include high speed and high performance machining technology, rotary ultrasonic precision machining technology, on-machine verification technology for NC machining accuracy, performance analysis and optimisation of manufacturing equipments. As PI, he has completed various national, provincial and industrial projects. He has published more than 200 research papers, applied patents, achieved software copyrights, and received national and provincial level scientific and technology awards several times.

Xiangyu Zhang is an Assistant Research Fellow in the Department of Mechanical Engineering, Tsinghua University Beijing, China. His research interests include high efficient and precision machining technology for difficult-to-cut materials (titanium alloys, super alloys, composites, etc.). He has published various papers and presented research in international conferences.

---

## 1 Introduction

Nomex honeycomb composites (NHCs) have been paid significant attention as a core material for various sandwich structures used in aerospace, military and automotive industries, owing to unique physical and mechanical properties such as high strength-to-weight ratio, low density, lightweight, corrosion resistant, excellent thermal insulations, energy absorption capability and flame retardant (Ahmad et al., 2020a; Pascoe et al., 2013; Dai et al., 2014; Roy et al., 2014; Liu et al., 2015; Ahmad et al., 2019). Sandwich structures mainly comprise face sheets of aluminium/CFRPs, NHCs core and adhesive bonding. NHCs core is primarily subjected to out-of-plane tensile and

compressive stresses whereas face sheets observe in-plane shear stress and tensile or compressive stress generated by bending. NHCs core is difficult to manufacture into complex curved parts by single moulding technique. Therefore, high quality machining is required to make NHCs core parts. But, high geometrical complexity, heterogeneous material properties, low density and thin-walled cellular structure of NHCs core makes it a difficult-to-machine material (Wang et al., 2019a; Asmael et al., 2021; Caggiano, 2018). Conventional machining produces significant processing defects such as large burr, tearing and uncut fibres, which limits large scale applications of NHCs core material. Durability and bonding strength of sandwich structures largely depends on the machining precision and surface quality of NHCs core. It has been reported in the literature that 5% NHCs core cells defects can cause 35% reduction of mechanical properties of sandwich structures (An et al., 2019). Therefore, in order to increase the bonding strength and durability of sandwich structure, the machined surface quality of NHCs core should be very high and precise. Various researchers have studied on different aspects of NHCs core machining such as Zarrouk (2020) studied on the various processing parameters in conventional machining of the NHCs and concluded that cutting forces increase with the increase in cutting depth whereas surface quality improves with the increase in spindle rotational speed. Ke et al. (2019) studied on the low machining efficiency and developed a high speed CNC milling force model and reveals that burr, tearing and uncut fibres observed by conventional machining. On the other hand, rotary ultrasonic machining (RUM) technology has been considered one of the most suitable method for high quality processing of various difficult-to-machine advanced materials such as alumina ceramic (Singh and Singhal, 2017, 2018a, 2018b, 2018c, 2018c), titanium alloys (Ti-6Al-4V) (Zhu et al., 2019), CFRPs composites (Wang et al., 2019b; Yakun et al., 2023), GFRP composites (Baraheni et al., 2019), C/SiC composites (Feng et al., 2017), and NHCs core (Liu et al., 2022; Zha et al., 2022) in order to mitigate the problems of conventional machining (large burr, tearing, uncut fibres, and delamination). In RUM process, owing to the advantages of periodic contact of tool with workpiece and impact action of the tool on the workpiece generated by ultrasonic vibration produces microcracks on the substrate surface which results in easy removal of material, high cutting efficiency and high surface quality. But, RUM applications for NHCs core processing are very limited on industrial scale due to complexity of the integrated RUM system, intricacy of RUM mechanism, specialised design of ultrasonic cutting tools, thin-walled lightweight cellular structure of NHCs and heterogeneous material properties and difficulty in processing parameters optimisation.

At present, very few studies found in the literature on RUM process of NHCs core such as Ahmad et al. (2020b) studied on the experimental investigations of RUM characteristics of NHCs core by ultrasonic circular disc tool, and concluded that NHCs processing with ultrasonic vibration gives good cutting quality and lower cutting force in contrast to no ultrasonic vibration of tool. Cao et al. (2020) developed a cutting force model for honeycomb material and experimentally verified that machining parameters values with high depth of cut and low width of cut gives good machining efficiency in terms of less burr and high surface quality. Yu et al. (2019) studied on the process path planning for rough and finish machining operations of honeycomb core in ultrasonic cutting of curved surfaces. Xia et al. (2019) investigated on the different design parameters of the ultrasonic disc tool and determined that rake angle of tool, radius of the tool and amplitude of vibration of the tool influenced significantly on the machining

efficiency of NHCs core. Xiang et al. (2018) performed a comparative study on the honeycomb core processing by ultrasonic longitudinal vibration and ultrasonic longitudinal-torsional vibration. The experimental results reveals that good machining quality can be achieved by using ultrasonic longitudinal-torsional vibration of the tool compared to longitudinal vibration only. Zha et al. (2022) studied on the ultrasonic disc tool wear characteristics based on radial difference calculation method for conventional and ultrasonic machining of NHCs material and concluded that ultrasonic machining can reduce tool wear by 36% compared to conventional machining under similar conditions. Kang et al. (2019) focused on the ultrasonic vibration cutting of NHCs core and obtained optimum value of oblique angle  $30^\circ$  and ultrasonic vibration amplitude  $25 \mu\text{m}$ .

Optimisation of processing parameters in RUM process of NHCs core is still quite confidential, time consuming, expensive and it must go through clear understanding of cutting force trends and cutting tool interaction with NHCs core surface during cutting process. But, due to special shaped cellular thin-walled structure of NHCs core, the interaction of cell walls with cutting edge of the circular tool varies. Moreover, it is highly challenging to get clear understandings of the workpiece-tool interaction during ultrasonic cutting experiments of NHCs core. Also, it is very complex and less accurate to realise the current challenges of NHCs core machining process. Besides that, processing parameters optimisation by experimental method is very costly, time consuming, and the mathematical modelling of such a complex cutting process does not give accurate results of all parameters. Therefore, researchers are more focused on the applications of finite element methods (FEM) and considering numerical modelling and simulation techniques as an alternative and best suitable method for comprehensive investigations on processing parameters and machining processes. Hence, study on the processing parameters optimisation by 3D FE cutting simulations was highly needed in order to understand and implement RUM process for NHCs core on large scale.

In the past, various researchers had focused on the finite element (FE) modelling and numerical simulations of difficult-to-machine materials such as carbon-fibre reinforced plastics (CFRPs) (Xu et al., 2021), glass-fibre reinforced plastics (GFRPs) (Quino et al., 2020) and honeycomb composite core (Zarrouk et al., 2021; Jaafar et al., 2017). NHCs core is one of the most studied honeycomb core material but heterogeneous material properties of NHCs core causes FE modelling and cutting simulations more challenging. Normally, the detailed core models can be more significant when material damage analysis is mainly concerned. Some of the studies found in the literature focuses on the impact modelling analysis by FE simulation such as Ivañez and Sanchez-Saez (2013) studied on the impact analysis of honeycomb core by using FE model implemented in ABAQUS/Explicit code. Audibert et al. (2019) performed FE modelling on ABAQUS/Explicit code for low-velocity impact test of sandwich composite with CFRP skins and Nomex honeycomb core. Buitrago et al. (2010) performed research on the perforations of NHCs core sandwich structures by 3D FE model implemented on ABAQUS/Explicit code. Whereas, very few studies were focused on the FE cutting simulations such as Sun et al. (2020) developed a 3D FE model for ultrasonic machining of aluminium honeycomb with circular disc tool on ABAQUS software based on Johnson-Cook (J-C) fracture model to reveal the ultrasonic machining mechanism and significant phenomena happening in the cutting process. Teng et al. (2018) conducted comparative study on the processing mechanism of micro/nano particles reinforced (SiC/Al) metal matrix composite using 3D FE modelling methods. Liu et al. (2017) developed a FEM simulations constitutive material model to study micro machining

mechanism as well as surface quality of CFRPs. Huang (2015) performed a research on the ultrasonic cutting mechanism of Nomex honeycomb core by considering the fracture mechanics for ultrasonic vibration assisted straight knife machining process.

NHCs core structure is mainly distinguished by orthotropic behaviour of material having high compression resistance of honeycomb core in the thickness direction (T-direction). The orthotropic nature of honeycomb material is mainly allied with NHCs core alveolar geometry and with the inherent nature of aramid paper (Zinno et al., 2011; Aminanda et al., 2009), which causes more complexity in the machining of NHCs core. Therefore, understanding of mechanical properties, processing parameters optimisation and material processing mechanism of NHCs core materials are much more complex than other traditional materials. Besides that, some researchers were focused to estimate the macroscopic NHCs behaviour by using meso-models. Majority of the studies found in the literature on 2D FE modelling approaches and very few of them were focused on the 3D FE modelling approaches. Giglio et al. (2012) conducted research on the NHCs core crushing behaviour by 2D and 3D elements and concluded that the 2D elements of NHCs core were capable to judge the preliminary failure of the honeycomb structure whereas, the 3D elements of NHCs core done well in the subsequent Plateau of the stress-strain curve. But 3D FE modelling is much more complex and high computational effort is required. The 3D FE model have the ability to simulate RUM process more precisely with cutting tool having very complex geometry and performance features. Studies on the RUM process optimisation of Nomex honeycomb core with circular disc tools in literature does not provide clear values of optimised machining parameters and cutting forces behaviour during RUM process. Therefore, it is of great significance to reveal the processing parameters optimisation by 3D FE cutting simulations of NHCs core material and to understand the behaviour of cutting forces in ultrasonic cutting process.

In this paper, a 3D FE ultrasonic cutting simulation model of NHCs core was developed for RUM process with an ultrasonic circular saw blade cutting tool to reveal the behaviour of cutting forces, processing parameters optimisation and chip formation. Hashin failure criteria was applied which is one of the most extensively used failure criteria for composite materials failure analysis as well as added in ABAQUS software. FE code ABAQUS/Explicit was used in order to develop 3D FE model and cutting simulations of NHCs core workpiece in ultrasonic machining process with circular disc tools. Finally, the 3D FE model of NHCs core was validated by performing various cutting experiments on ultrasonic machine tool and optimised set of processing parameters was revealed.

## **2 3D FE modelling and cutting simulations of NHCs core**

### *2.1 Material damage models for FE cutting simulations*

Material damage model describes the origination criteria and related laws of damage progression in cutting simulation processes of difficult-to-machine materials. In the cutting simulation technology, when the material failure phases are achieved, FE software uses relevant damage evolution laws to find the degradation of material. Precision of material damage model and constitutive material model have significant influence on the FE cutting simulation results. Therefore, development of an accurate material damage model in accordance with material geometry and mechanical properties

is a key technique in the machining simulations for RUM process of difficult-to-machine materials. The term failure criterion states the mathematical equations that predict the conditions of stress and strain at the onset stage of damage. Various material damage models have been reported on FE cutting simulations of different materials such as J-C model (Wang et al., 2018), Tsai Wu failure criteria (Li et al., 2019), shear deformation model (Razanica et al., 2020), 3D FE coupled Eulerian-Lagrangian (CEL) model (Peng et al., 2019) and Hashin damage model (Wang et al., 2021). Moreover, there are three types of failure criteria; interactive failure criteria, non-interactive failure criteria and separate mode failure criteria. In order to determine the interaction between various stresses, the interactive failure criteria are used, Tsai Wu and Tsai Hill are the common examples of this type of failure criteria. Non-interactive failure criteria fall in the second category which is further categorised as maximum stress law and the strain criterion. Both of these criteria are easy to understand and can predict directly the failure of the composites material when either stress or strain exceeds the maximum allowable limit. Separate mode failure criteria are the third failure criteria to predict failure mode of composite materials and key example is Hashin damage model.

Hashin damage model has been considered most suitable for the fibre-reinforced composite materials. Typically, Hashin failure criteria is used to find the damage directions and failure modes of every element which permits to analyse the rigidity on every increment (Gawryluk and Teter, 2021). Hashin proposed this criterion in order to forecast various composite materials failure based on the damage mechanisms instead of being an extrapolation of the already existing criterion for other materials (Xiong et al., 2018). This criterion interacts with more than one stress components to evaluate various fracture modes. There are four various modes of failure in Hashin's criterion for composite materials; fibre tension, fibre compression, matrix tension and matrix compression as described in the following equations (Wang and Melly, 2017):

- Fibre tension  $\sigma_{11} \geq 0$ :

$$\left(\frac{\sigma_{11}}{X_T}\right)^2 + \frac{\sigma_{12}^2 + \sigma_{13}^2}{S_{12}^2} = \begin{cases} \geq 1 & \text{Failure} \\ < 1 & \text{No failure} \end{cases} \quad (1)$$

- Fibre compression  $\sigma_{11} < 0$ :

$$\left(\frac{\sigma_{11}}{X_C}\right)^2 = \begin{cases} \geq 1 & \text{Failure} \\ < 1 & \text{No failure} \end{cases} \quad (2)$$

- Matrix tension  $\sigma_{22} + \sigma_{33} > 0$ :

$$\frac{(\sigma_{22} + \sigma_{33})^2}{Y_T^2} + \frac{\sigma_{23}^2 - \sigma_{22}\sigma_{33}}{S_{23}^2} + \frac{\sigma_{12}^2 + \sigma_{13}^2}{S_{12}^2} = \begin{cases} \geq 1 & \text{Failure} \\ < 1 & \text{No failure} \end{cases} \quad (3)$$

- Matrix compression  $\sigma_{22} + \sigma_{33} < 0$ :

$$\left[\left(\frac{Y_C}{2S_{23}}\right)^2 - 1\right] \left(\frac{\sigma_{22} + \sigma_{33}}{Y_C}\right) + \frac{(\sigma_{22} + \sigma_{33})}{4S_{23}^2} + \frac{\sigma_{23}^2 - \sigma_{22}\sigma_{33}}{S_{23}^2} + \frac{\sigma_{12}^2 + \sigma_{13}^2}{S_{12}^2} = \begin{cases} \geq 1 & \text{Failure} \\ < 1 & \text{No failure} \end{cases} \quad (4)$$

where  $\sigma_{ij}$  are the stress component and  $T$  and  $C$  represents the tensile and compressive strengths of the laminate,  $X_T$ ,  $Y_T$ ,  $X_C$ ,  $Y_C$  shows the allowable tensile strengths and allowable compressive strengths respectively. Whereas,  $S_{12}$ ,  $S_{13}$  and  $S_{23}$ , denotes allowable shear strengths.

## 2.2 3D modelling and FE cutting simulations of NHCs core

In this study, FE code ABAQUS/Explicit was used for 3D modelling and simulations of Nomex honeycomb material in RUM process with circular disc tool. Fundamental behaviour laws were applied via user defined subroutine VUMAT in ABAQUS/Explicit software. Precise material basic model is the most important technique for 3D FE modelling and machining simulation in RUM process of NHCs core. The material constitutive model in 3D FE modelling and simulation largely depends on the geometric features of the workpiece and material properties. In this paper, NHCs core workpiece is used having density 48 kg/m<sup>3</sup>, cell size 3.2 mm and regular hexagonal cellular structure. Key geometric features and mechanical properties of NHCs core workpiece (Jaafar et al., 2017, 2021) for 3D FE modelling and ultrasonic cutting simulations are mentioned in Table 1.

**Table 1** NHCs core mechanical properties and geometric features for 3D FE modelling and simulation

<i>Material property</i>	<i>Value</i>
Longitudinal tensile strength	111 [MPa]
Longitudinal compressive strength	53 [MPa]
Transverse tensile strength	98 [MPa]
Transverse compressive strength	47 [MPa]
Longitudinal shear strength	59 [MPa]
Elastic modulus in machine direction (L-direction)	9,200 [MPa]
Elastic modulus in cross direction (W-direction)	8,300 [MPa]
Elastic modulus in out-of-plane direction (T-direction)	4,700 [MPa]
Shear modulus in L-W direction	2,600 [MPa]
Shear modulus in L-T direction	1,700 [MPa]
Shear modulus in W-T direction	1,700 [MPa]
Poisson's ratio ( $\nu_{12}$ , $\nu_{13}$ , $\nu_{23}$ )	0.35
Density	48 [Kg/m <sup>3</sup> ]
Cell size ( $D$ )	3.2 [mm]
Cell wall length ( $l$ )	1.83 [mm]
Single wall thickness ( $t$ )	0.065 [mm]
Cell wall angle ( $\alpha$ )	120°

In order to analyse the interactional behaviour of NHC material and ultrasonic circular disc tool, the 3D FE model of NHCs core structure was composed by  $9 \times 7$  cells-rows as shown in Figure 1(a). NHCs material core was 3D modelled by applying shell elements with hour glass control and element deletion, reduced integration and four-node linear elements of S4R type. The mesh element size for NHCs core workpiece was taken

2.5  $\mu\text{m}$  and the developed 3D model considers the orthotropic properties of NHCs core material. Owing to the hexagonal cellular structure of NHCs core, the 3D FE model has large complexity and required high computational effort and time for cutting simulations. Therefore, in order to avoid the high complexity and long computational time, partition methodology with datum plane was used to develop 3D FE model in which cutting region of the workpiece was modelled with smaller element size and rest of the workpiece with bigger elements size as shown in Figure 1(b).

**Figure 1** NHCs core hexagonal cellular structure and 3D FE model for cutting simulation (see online version for colours)

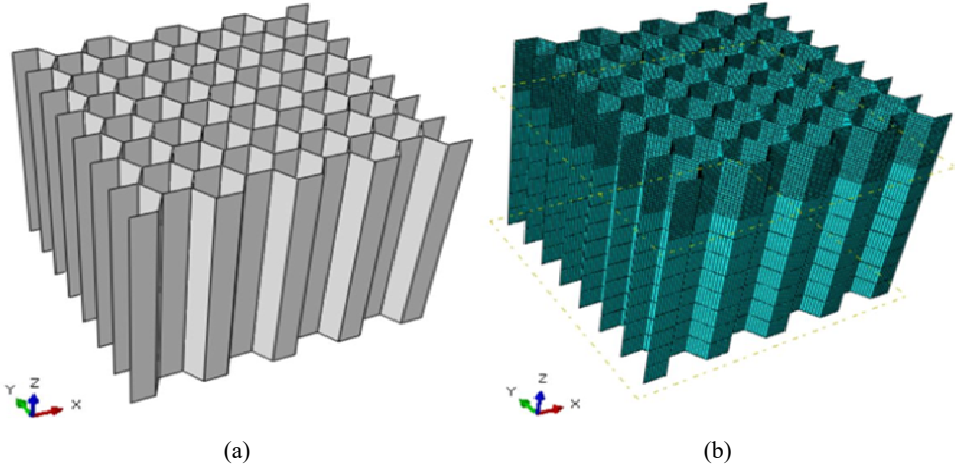
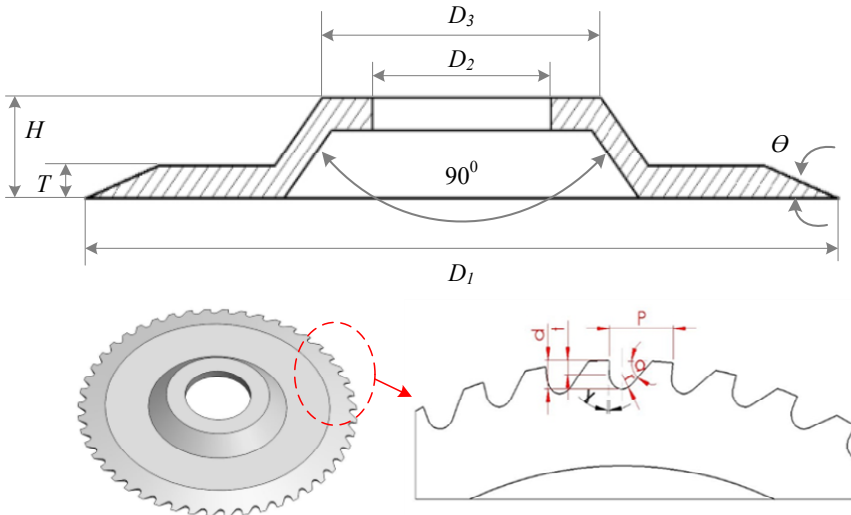


**Figure 2** Schematics of specialized UCSB tools (see online version for colours)



Source: Ahmad et al. (2020b)

In 3D FE model, the adhesive material between the cell walls was ignored due to very high bonding strength and it was supposed that no adhesive failure occurs during cutting

of NHCs core by RUM process. In this investigation, a novel UCSB tool was used for 3D FE modelling and cutting simulation of NHCs core. The material of UCSB cutting tool used in 3D FE modelling is high-speed steel (HSS). Since the stiffness of the ultrasonic circular knife type cutting tool is higher compared to NHCs core. Therefore, the cutting tool was considered a rigid body having negligible deformation and also tool wear in the machining process was ignored. Owing to the complexity of the ultrasonic cutting tools structure, 3D model of the specialised cutting tools was developed on Solidworks software and imported in FE code ABAQUS/Explicit. The schematics of the specialised cutting tool is shown in Figure 2.

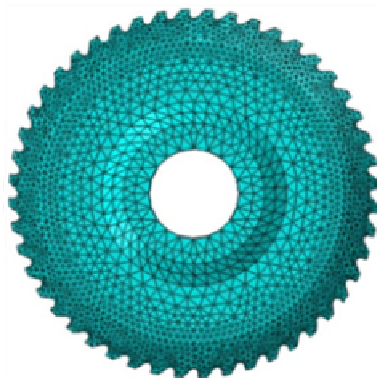
As shown in Figure 2, key design parameters of specialised UCSB tool are maximum diameter ( $D_1$ ), diameter of horn fitting hole ( $D_2$ ), diameter of top face ( $D_3$ ), tool thickness ( $T$ ), tool height ( $H$ ), wedge angle ( $\Theta$ ), pitch of the saw teeth of the tool ( $P$ ), the gullet radius of the saw teeth ( $r$ ), side clearance angle ( $\alpha$ ), rake angle of the saw teeth ( $\gamma$ ) and tooth depth ( $d$ ). The values of key geometrical parameters of specialised UCSB tool are mentioned in Table 2.

**Table 2** Values of the key geometrical parameters of specialised UCSB tools

<i>Geometrical parameters</i>	<i>Values</i>
Maximum diameter ( $D_1$ )	27 mm
Angle of wedge ( $\Theta$ )	17°
Dia. of the horn fitting hole ( $D_2$ )	6.40 mm
Dia. of the top face ( $D_3$ )	10 mm
Thickness of the tool ( $T$ )	0.90 mm
Height of the tool ( $H$ )	2.70 mm
UCSB tool saw teeth	48

*Source:* Ahmad et al. (2020b)

**Figure 3** 3D FE model of specialised UCSB tool (see online version for colours)



The targeted resonant frequency of the tool designed in this study was  $\geq 20$  kHz. The mesh employed on cutting tool in this research was four-node linear tetrahedral elements of type C3D4 which is typically used for 3D stress elements. 3D FE model of the

specialised UCSB tool was applied in the ultrasonic cutting simulations process as shown in Figure 3.

In 3D FE modelling and simulations process, the cutting tool was represented with reference point situated at centre of its revolution axis. The ultrasonic processing conditions were assigned to tool through a specified reference point and feed rate in Y-direction, spindle speed (rpm) and vibration amplitude in Z-axis. In the ultrasonic cutting simulations process, the load and boundary conditions constraints according to actual working conditions necessarily are applied to the cutting tool and the NHCs material. In terms of the boundary conditions, conventional methods of holding the NHCs core workpiece have more complexities owing to the weak local strength of NHCs material. However, in the actual machining process, the NHCs core workpiece was fixed with double sided adhesive tape attached on the steel plate. But, 3D FE model was assumed as held firmly in cutting simulations and all the bottom joints of the NHCs core workpiece were fully fixed with boundary conditions applied in the load module (ENCASTRE,  $U1 = U2 = U3 = UR1 = UR2 = UR3 = 0$ ). In the RUM process of NHCs core, ultrasonic circular knife cutting tool mainly involves three motions relative to the workpiece of honeycomb core material such as feed movement in the direction of x-axis or y-axis, circular disc tool rotary movement along its cutting trajectory and tool vibratory motion with the spindle axis in z-direction. Therefore, in order to apply boundary conditions on tool, the velocity/angular velocity was employed on tool in ABAQUS software; feed velocity (V1) along y-axis and rotary motion of the tool (VR3) along z-axis. Whereas, ultrasonic vibratory motion of the tool in reciprocating mode was applied in the z-direction to the periodic amplitude function of the Fourier series. The equation for ultrasonic vibration at any node of ultrasonic cutting tool during RUM of NHCs core along z-axis of the tool can be described as:

$$Z_i = A \sin(2\pi ft) \quad (5)$$

Here,  $A$  is ultrasonic vibration amplitude ( $\mu\text{m}$ ) of the tool,  $f$  is resonant frequency (Hz) of the tool and  $t$  is time (sec). Moreover, the periodic amplitude function in the mathematical formula can be stated with Fourier series which is also added in the ABAQUS software and expressed in the equation 6.

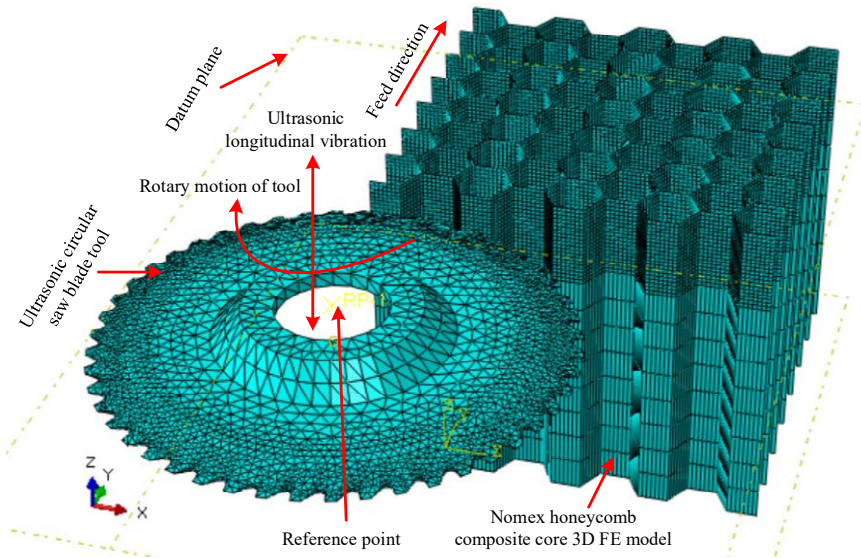
$$a = A_0 + \sum_{n=1}^N [A_n \cos n\omega(t - t_0) + B_n \sin n\omega(t - t_0)] \quad (6)$$

where  $A_0$  is initial vibration amplitude ( $\mu\text{m}$ ),  $\omega$  is angular frequency (rad/sec),  $A_n$  is the coefficient of cos function and  $B_n$  is the coefficient of sin function. The 3D FE cutting simulation model of NHCs core for RUM process by UCSB tool is shown in Figure 4.

In 3D FE model, contact interface of the cutting tool with NHCs core workpiece was stated through surface-to-surface contact method and with penalty contact method. Besides that, interaction among honeycomb cell walls was assigned by the general contact with penalty contact method. In this study, mechanical contact method was used whereas hard contact is used for normal contact and Coulomb law is used for tangential contact. Furthermore, the contact between the surface of circular disc cutting tool and NHCs core nodes in the each ultrasonic vibration cycle must be confirmed and the impact of ultrasonic vibration can be stated during ultrasonic cutting simulations process. If 3D FE model have large number of elements then the CPU time will be longer which have no significant advantage on targeted outcomes of the ultrasonic cutting simulation

process. Therefore, to reduce computational time of NHCs material 3D FE model by considering the vibration amplitude of the cutting tool and balance among the computational time and desired results, a finer mesh with smaller elements was implemented as shown in Figure 4. The main purpose of developing 3D FE model and cutting simulation of NHCs core structure in RUM by novel ultrasonic circular saw blade knife type cutting tool was to understand the interaction between the NHCs core structure and cutting force behaviour during RUM process, and to optimise the processing parameters of NHCs core. Therefore, in order to investigate the phenomena during RUM process of NHCs core and influence of various processing conditions such as feed rate, spindle speed and vibration amplitude on cutting force, a number of cutting simulations were performed on ABAQUS/Explicit dynamic software with the developed 3D FE model. The cutting forces ( $F_x$  and  $F_y$ ) obtained by 3D FE ultrasonic cutting simulations for UCSB cutting tool are illustrated in Figure 5. The cutting force graph of 3D FE cutting simulations for UCSB cutting tool shows variations due to the cellular structure of workpiece, heterogeneous material properties and contact relation of the circular knife type cutting tool varies continuously. Therefore, an average value of the cutting force from the FE cutting simulation graph was selected against each set of processing parameters for the final results.

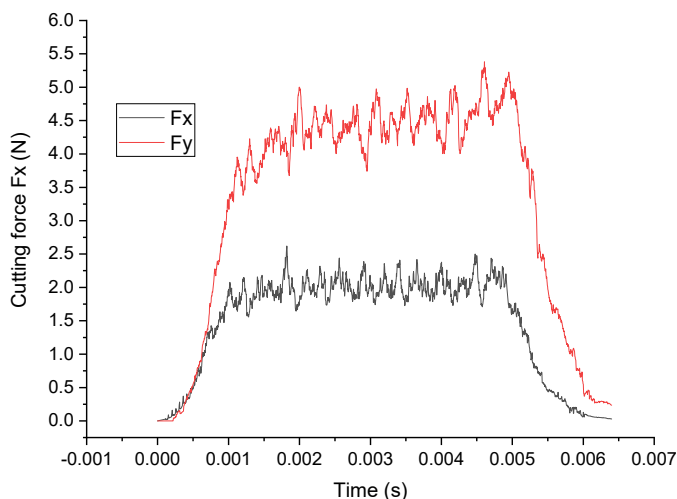
**Figure 4** 3D FE cutting simulation model of NHCs core for RUM process by UCSB tool (see online version for colours)



As shown in Figure 5, the cutting force  $F_x$  is lower than  $F_y$  under similar processing parameters in RUM of NHCs core. Cutting force  $F_x$  at initial phase of cutting process is very low between time 0.000 to 0.001 seconds but it starts increasing dramatically between the time 0.001 to 0.002 seconds which is the cutting phase of the RUM process. Fewer variations in the cutting force  $F_x$  occurred in the time range of 0.002 to 0.005 seconds as it is the material removing phase and then the cutting force reduced in the final phase. Figure 5, also depicts the cutting force  $F_y$  obtained by FE ultrasonic cutting simulations of NHCs core. Cutting force  $F_y$  starts increasing quickly between the time

range 0.000 to 0.001 seconds and reaches at 4N then it remains stable between 0.001 to 0.005 seconds with minor fluctuations due to cellular structure of the workpiece. But cutting force  $F_y$  decline sharply from 0.005 to 0.006 seconds as it is the cutting tool exit phase from the workpiece material. Finally, cutting force ( $F_x$  and  $F_y$ ) results against each cutting test were depicted by the simple line graphs because there were number of processing factors involved and multiple set of processing parameters were used in the FE cutting simulations analysis. Accordingly, the final results were simplified by line graphs to see the cutting force trends against each set of processing parameters.

**Figure 5** Cutting force ( $F_x$  and  $F_y$ ) by FE cutting simulations in RUM of NHCs core (see online version for colours)

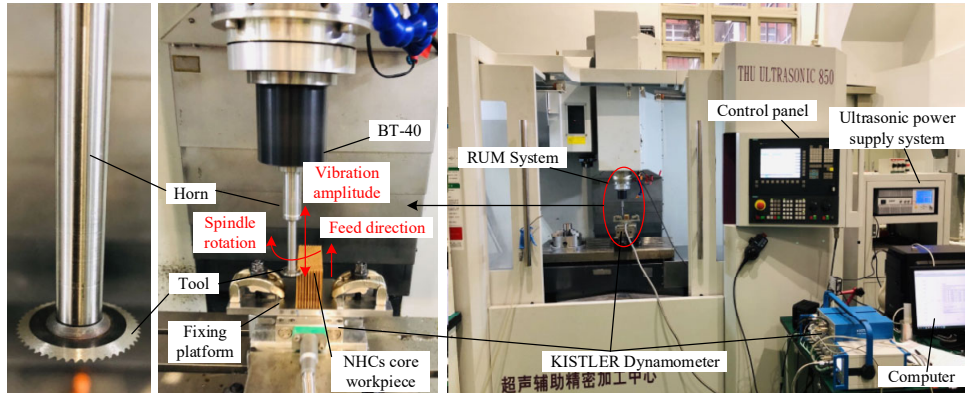


### 3 Experimental scheme

Number of experiments under different ultrasonic processing conditions were conducted to study the accuracy of 3D FE model, ultrasonic cutting simulations of NHCs core workpiece and to find optimum processing parameters. Hexagonal cellular structure of NHCs core workpiece having dimensions as length ( $L = 80$  mm), width ( $W = 30$  mm), and height ( $H = 30$  mm) was used in ultrasonic machining experimental study. In this study, two sided adhesive bonding tape was applied to fix the experimental workpiece of NHCs core on the steel plate which was further clamped on cutting force gauge Kistler dynamometer and also with fixture platform on the machine table. Experimental setup for ultrasonic machining of honeycomb core material with ultrasonic disc cutting tools primarily includes an ultrasonic spindle system linked with BT40 which is a standard tool holder, a CNC machine tool along with computer to get the experimental results, BP4610 a high-speed bipolar ultrasonic power supply system, a compensation capacitor having high-frequency, an ultrasonic acoustic vibration system with integrated transducer and horn, ultrasonic circular disc tool, fixture platform, a KISTLER Dynamometer which was used to measure cutting force. Key functional parameters of rotary ultrasonic machine tool includes  $\geq 20$  kHz resonant frequency,  $27 \mu\text{m}$  maximum vibration amplitude of the integrated system, 2 kW ultrasonic power, 10,000 rpm spindle speed. In this research,

experimental work was done on THU Ultrasonic 850 which was established by Tsinghua University China. Moreover, each experiment was done periodically three times and finally the average results of cutting force were selected to achieve most appropriate results. Experimental setup used for this study is shown in Figure 6.

**Figure 6** Experimental setup for ultrasonic machining of honeycomb core materials (see online version for colours)



In this research, self-designed ultrasonic circular saw blade (UCSB) cutting tool was used in the RUM experimentation work on NHCs core workpiece, tool parameters are shown in Table 2, and fabricated tool shown in Figure 7.

**Figure 7** Self-designed UCSB cutting tools used in RUM experiments of NHCs core (see online version for colours)

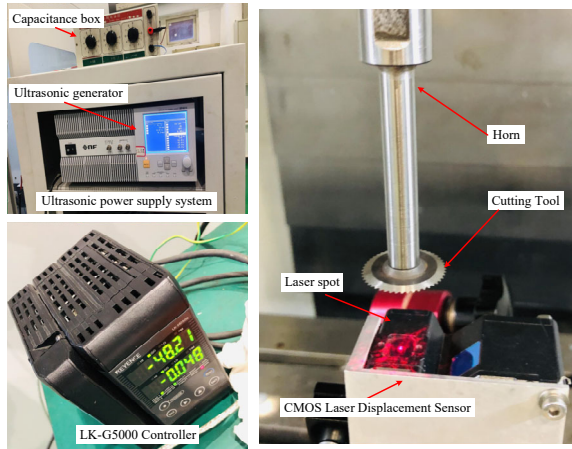


Source: Ahmad et al. (2020b)

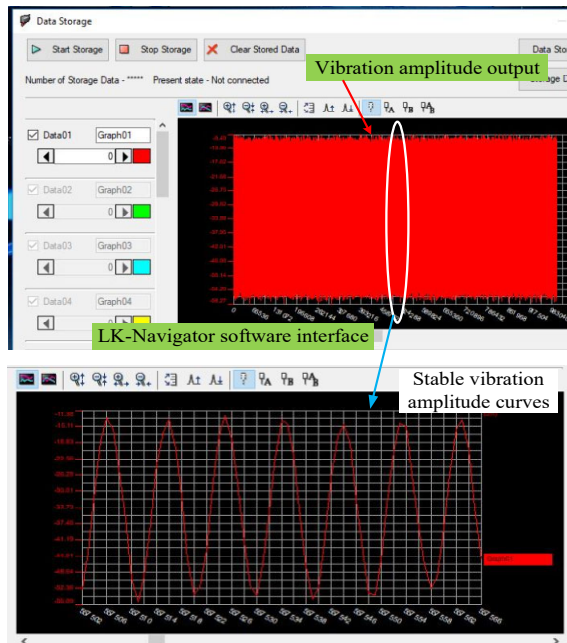
The experimental procedure initially includes the identification of ultrasonic resonant frequency of integrated structure of rotary ultrasonic processing system with control knob of bipolar ultrasonic power supply system BP4610. The experimentally measured ultrasonic resonant frequency was 22,050 Hz. The measured resonant frequency was closer to the designed resonant frequency  $\geq 20$  kHz and good enough to perform NHCs core cutting experiments. Secondly, ultrasonic vibration amplitude was measured against various values of voltage by using CMOS laser displacement sensor LK-H020 with

controller KEYENCE LK-G5000 series and LK-Navigator software interface (Liu et al., 2022). The laser displacement sensor was fixed over the machine table and a specific distance was maintained between the cutting tool edge and laser sensor so that laser spot strikes on the cutting edge of the circular disc cutting tool and LK-G5000 controller shows value near to zero as shown in Figure 8.

**Figure 8** Setup for measurement of vibration amplitude and output data recorded on LK-navigator software interface, (a) vibration amplitude test apparatus (b) vibration amplitude output data (see online version for colours)



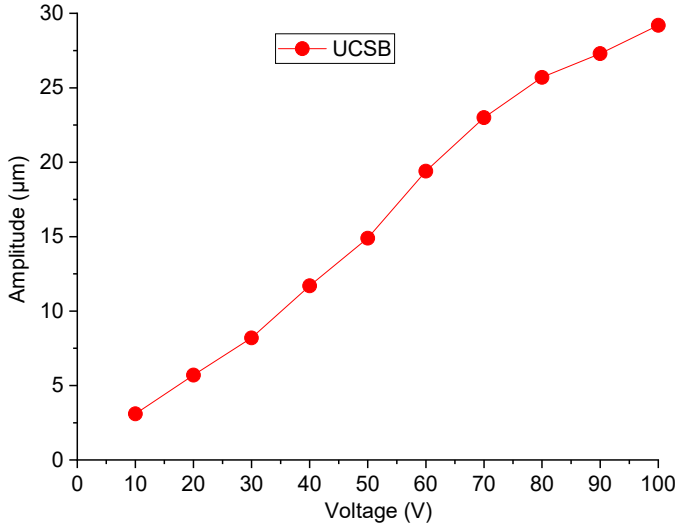
(a)



(b)

As described in Figure 8, the output data of vibration amplitude was recorded at resonant frequency 22,050 Hz of UCSB cutting tool against the voltage values from 10 V to 100 V in series of ultrasonic experiments. Moreover, in this study, experiments to measure amplitude were repeated three times and average value of the amplitude was selected at 20–25 stable vibration amplitude curves (Ahmad et al., 2020b). The ultrasonic experimental results of vibration amplitude against voltage values are shown in Figure 9.

**Figure 9** Vibration amplitude values of UCSB cutting tool against voltage (see online version for colours)



In the RUM process, Kistler dynamometer was used to measure the cutting force  $F_y$  and  $F_x$ . Signals of the measured cutting forces received from Kistler dynamometer were amplified by a charge amplifier and further recorded by a data acquisition card. The data recorded in the acquisition card exhibits the direct current component of the actual cutting force which is independent of the sampling frequency and natural frequency of the Kistler dynamometer. Therefore, the average values of cutting force signifies the most appropriate index to measure and compare the RUM performance of NHCs core workpiece. Figure 10 shows graphical representation of the measured cutting force versus time and the average value of cutting force  $F_c$  can be calculated as (Ahmad et al., 2020b):

$$F_c = \frac{1}{t_2 - t_1} \int_{t_1}^{t_2} F dt \quad (7)$$

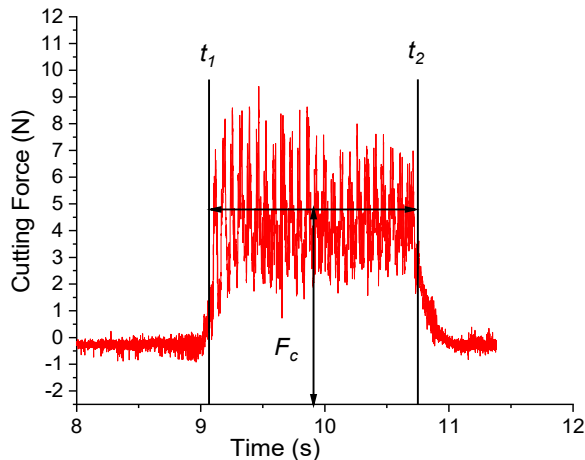
where  $F_c$  is average cutting force,  $t_1$  and  $t_2$  are the machining time when circular cutting tool starts and ends the cutting process of NHCs core workpiece, respectively.

#### 4 Results and discussion

The main purpose to develop 3D FE model and cutting simulation of NHCs core structure in RUM process with new UCSB tool was to understand the interaction between

the NHCs core structure and cutting forces behaviour during RUM process, and to optimise the processing parameters of NHCs core. Therefore, in order to study phenomena during RUM process of honeycomb material and effect of various machining conditions, the developed 3D FE model was verified by performing several experiments on ultrasonic machine tool under same processing conditions as in cutting simulations and comparison of processing results was obtained.

**Figure 10** Cutting force measured by Kistler dynamometer versus time curve of NHCs core (see online version for colours)



Source: Ahmad et al. (2020b)

#### 4.1 3D FE ultrasonic cutting simulation model validation

To confirm results of 3D FE model, cutting forces ( $F_x$  and  $F_y$ ) average values along machining directions achieved by running FE simulations on ABAQUS dynamic explicit software were compared with the experimentally measured data. One of the significant factor that reflect the optimisation of processing parameters in the machining of difficult-to-machine materials is the cutting force. Therefore, in this study, the trends of cutting forces were mainly considered to assess the influence of various set of processing parameters of NHC core material during RUM process by new UCSB tool. In conventional materials the cutting force is typically considered from three aspects; the elastoplastic materials deformation resistance, frictional resistance among rake face of tool and chips formed, and thirdly machined surface and flank face undergoes extrusion and friction. But permanent deformation of composite materials such as NHCs core was not clear during machining process and very thin thickness of the NHCs core cell wall makes extrusion and friction insignificant along machined surface and cutting tool. Due to heterogeneous material properties of NHCs core, theoretical model development of cutting force has more complexities and very challenging. Therefore, a 3D FE model was developed and numerical cutting simulations and actual experimental tests were performed with fixed values of resonant frequency 22,050 Hz, cutting width 8 mm and cutting depth 2 mm under the same cutting conditions to measure trends of cutting forces ( $F_x$  and  $F_y$ ). Processing conditions for numerical cutting simulations and experimental tests of NHCs core by RUM process are described in Table 3.

**Table 3** Processing conditions for numerical simulations and experimental tests of NHCs core by RUM process

<i>Test type</i>	<i>Variable parameters</i>	<i>Fixed parameters</i>
Vibration amplitude ( $\mu\text{m}$ )	05, 10, 15, 20, 25, 27	Spindle speed 3,000 rpm, feed rate 500 mm/min
Spindle speed (rev./min)	1,000, 2,000, 3,000, 4,000, 5,000	Amplitude 25 $\mu\text{m}$ , feed rate 500 mm/min
Feed rate (mm/min)	500, 1,000, 1,500, 2,000, 2,500, 3,000	Spindle speed 3,000 rpm, amplitude 25 $\mu\text{m}$

NHCs core workpiece has weak rigidity along width and length which produces large deformation of honeycomb core cellular structure. Whereas, strong rigidity exists along thickness which yields slight deformation in NHCs core during machining. Therefore, the cutting force  $F_z$  shows no substantial effect on machining performance in terms of surface quality and precision of workpiece. Conversely, if the cutting force along width and length ( $F_x$  and  $F_y$ ) is too high, the workpiece will undergoes high cutting resistance and large material deformation. Current research mainly focuses on three types of numerical and experimental tests in ultrasonic machining of Nomex honeycomb core workpiece with newly developed UCSB cutter to study the impact of cutting parameters on machining performance in terms of cutting force ( $F_x$  and  $F_y$ ) such as amplitude test in which ultrasonic vibration amplitude changed from 5  $\mu\text{m}$  to 27  $\mu\text{m}$ , feed rate test having range of feed rate from 500 mm/min to 3,000 mm/min, and spindle speed test with values of spindle speed from 1,000 rpm to 5,000 rpm as described in Table 3. FE cutting simulations and experimental results of RUM process on NHCs core for three types of cutting tests are discussed in sections below.

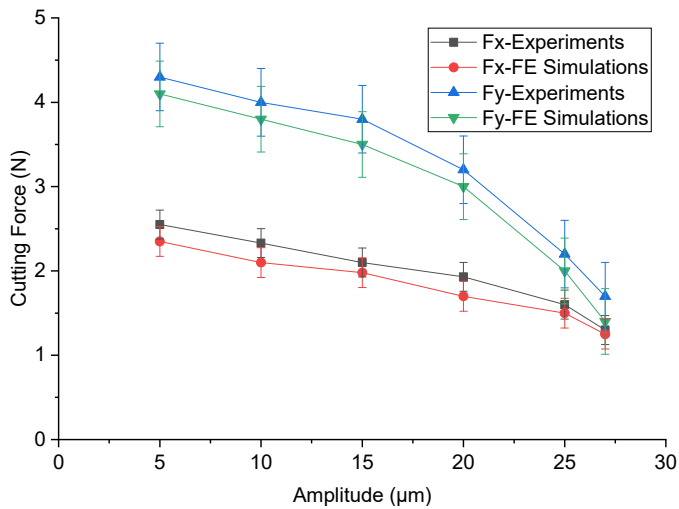
#### 4.1.1 Ultrasonic vibration amplitude impact on cutting force

In the first ultrasonic cutting experiment on NHCs core workpiece, impact of amplitude on cutting forces ( $F_x$  and  $F_y$ ) was analysed by changing the amplitude value from 5  $\mu\text{m}$  to 27  $\mu\text{m}$  and keeping all other processing parameters constant; feed rate 500mm/min, depth of cut 2 mm, spindle speed 3,000 rpm and cutting width 8 mm. Vibration amplitude was adjusted with respect to voltage value of the RUM system in the actual cutting experiments whereas in numerical simulations the vibration amplitude value was used directly in the ABAQUS software. All the experiments were repeated three times and average values of the cutting forces were used in the final results. RUM experiments and FE simulations results are presented in Figure 11.

There is a decreasing trend in cutting force ( $F_x$  and  $F_y$ ) in response to increase in amplitude during ultrasonic machining process of NHCs core material with novel UCSB cutting tool as displayed in Figure 11. Initially, there was a slight decrease in cutting force ( $F_x$  and  $F_y$ ) at amplitude from 5  $\mu\text{m}$  to 10  $\mu\text{m}$ . However, at higher vibration amplitude from 10  $\mu\text{m}$  to 25  $\mu\text{m}$ , there was a significant decrease in cutting force ( $F_x$  and  $F_y$ ) because of high cracks development in workpiece due to high vibrational impact force of ultrasonic disc cutter. Cutting force  $F_y$  is typically high compared to  $F_x$  because of feeding direction and faces main resistance during cutting whereas,  $F_x$  is material removal force which removes material from machined surface. Less cutting force was observed while ultrasonic machining with new UCSB tool due to shorter contact surface

of tool with substrate surface (workpiece) and also there was enough teeth gap at cutting edge. As presented in Figure 11, cutting force ( $F_x$  and  $F_y$ ) obtained by 3D FE modelling and simulation was slightly lower than the actual RUM experiments because of environmental factors, RUM equipment handling errors, NHCs core material property variations and manufacturing defects, and ultrasonic cutting tools manufacturing flaws with respect to precision and cutting tool material properties accuracy. Both 3D FE cutting simulations and RUM experimental results shows that newly established 3D FE ultrasonic machining model is valid to foresee cutting force ( $F_x$  and  $F_y$ ) in RUM process of Nomex honeycomb core materials and can be helpful in cutting tools design optimisation and to get optimum ultrasonic processing of NHC core. The vibration amplitude 25  $\mu\text{m}$  is considered optimum and most appropriate because of lowest cutting force ( $F_x$  and  $F_y$ ) value and further increase in the value of vibration amplitude can cause the RUM system heating and more material damages.

**Figure 11** Amplitude impact on cutting force ( $F_x$  and  $F_y$ ) (see online version for colours)



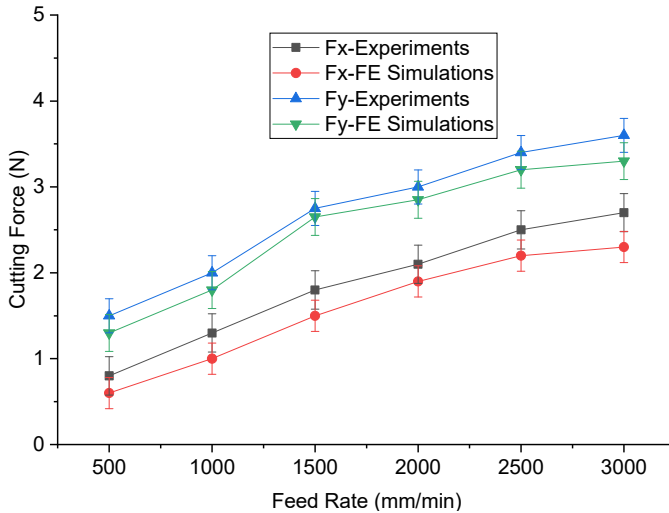
#### 4.1.2 Feed rate impact on cutting force

In order to reveal the impact of feed rate on machining performance in terms of machined surface quality and cutting force ( $F_x$  and  $F_y$ ), ultrasonic machining experiments on Nomex honeycomb core material and numerical simulations on ABAQUS dynamic explicit software were performed. Ultrasonic machining parameters for experimental and simulation work includes; feed rate from 500 mm/min to 3,000 mm/min, amplitude 25  $\mu\text{m}$ , spindle speed 3,000 rpm, width of cut 8 mm and depth of cut 2 mm. Vibration amplitude value was adjusted in correspondence to voltage of ultrasonic system. 3D FE ultrasonic cutting simulation and RUM experimental results are presented in Figure 12.

As depicted in Figure 12, there is a direct relation of feed rate with cutting force such as cutting force ( $F_x$  and  $F_y$ ) increases with the increase in feed rate in ultrasonic machining of Nomex honeycomb core material with new UCSB cutting tool due to increase in volume of material removed per unit time. 3D FE modelling and simulations results of cutting force ( $F_x$  and  $F_y$ ) shows very small variations with actual RUM

experiments because of factors mentioned above in the amplitude test. Moreover, the penetration of tool in workpiece is high due to sharp saw teeth of UCSB tool which becomes one of the reason for lower cutting force. The feed rate 500 mm/min was considered optimum and most appropriate due to lowest cutting force ( $F_x$  and  $F_y$ ) value and further increase in the value of feed rate can cause more cutting resistance and more material damages.

**Figure 12** Feed rate impact on cutting force ( $F_x$  and  $F_y$ ) (see online version for colours)



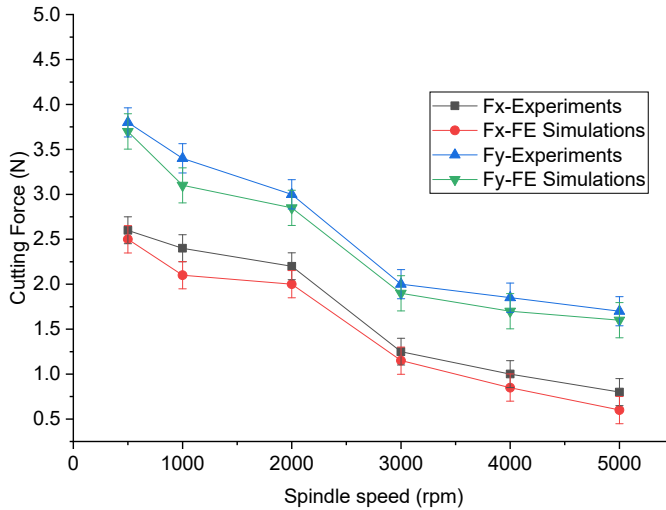
#### 4.1.3 Spindle speed impact on cutting force

The third type of test was performed to validate the 3D FE model of NHCs core workpiece by spindle speed variations effect on the cutting force. Both numerical cutting simulations and RUM experimental tests were conducted under RUM process conditions with spindle speed value from 1,000 rpm to 5,000 rpm and constant other processing parameters such as feed rate 500 mm/min, amplitude 25  $\mu\text{m}$ , width of cut 8 mm and depth of cut 2 mm. Vibration amplitude value was adjusted same as mentioned in amplitude test and feed rate test. All experiments were performed thrice under RUM process conditions and average value of cutting force was selected in the final results as shown in Figure 13.

Figure 13 depicts that there is a decreasing trend in cutting force ( $F_x$  and  $F_y$ ) when spindle speed increases under the conditions of RUM process with new UCSB ultrasonic tool in 3D FE simulations as well as actual ultrasonic machining experimental work on Nomex honeycomb core workpiece. Because increase in spindle speed causes to increase kinetic energy of ultrasonic circular disc tools which becomes the reason for lower cutting force and high rate of material removal. Saw cutting teeth in UCSB tool have less area of contact with substrate surface of workpiece in each cut which generates less machining friction in cutting region as well as lower thermal damages. Consequently, cutting force with UCSB tool is lower during RUM process of Nomex honeycomb core material. Figure 13 shows that cutting force obtained by 3D FE modelling and simulation does not shows much variations with the actual experiments results. Therefore, the

developed 3D FE model is valid and good enough to predict the cutting force and processing mechanism analysis. The spindle speed 3,000 rpm is considered optimum and most suitable due to lowest cutting force ( $F_x$  and  $F_y$ ) value as shown in Figure 13, and higher spindle speed leads to heating of RUM system.

**Figure 13** Spindle speed impact on cutting force ( $F_x$  and  $F_y$ ) (see online version for colours)

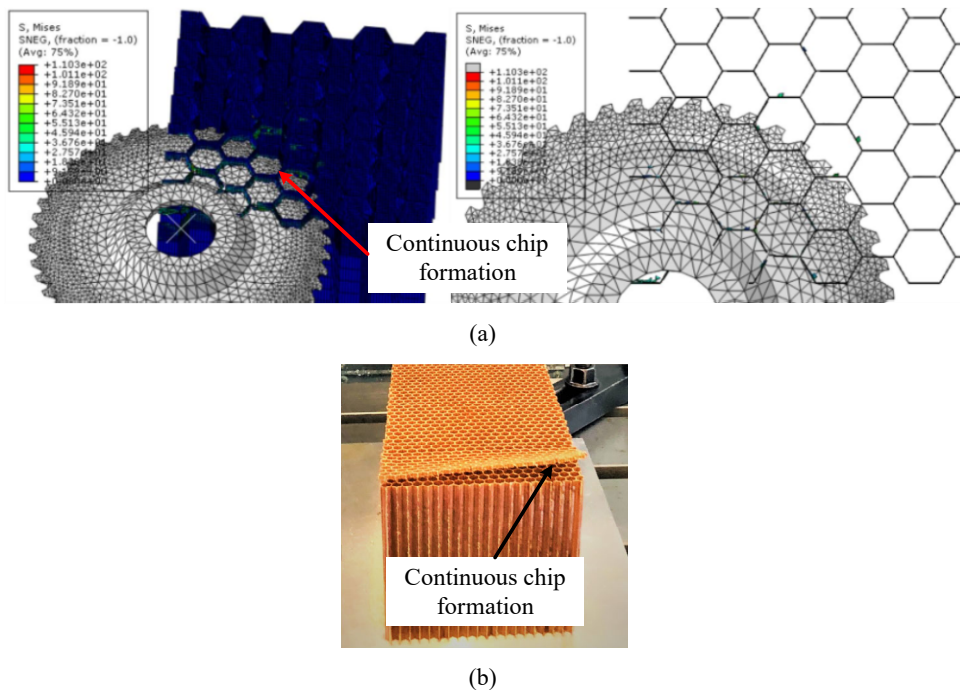


#### 4.2 Chips formation mechanism of NHCs core in RUM process

The fracture characteristics of NHCs core in ultrasonic machining with circular disc type tools is really problematic such as intermittent contact of ultrasonic tool with NHCs core workpiece generates impact fracture, extrusion of material produces plastic tensile fracture and edge of tool in whole cutting process causes shear fracture. In RUM process of NHCs core with circular disc tools, the shear fracture always exists. Microcracks developed in the cell wall before the cutting tool reaches the initial contact position with workpiece during RUM process because impact action caused by ultrasonic vibration amplitude of the tool. Moreover, interface of cutting tool with workpiece material is the most significant factor involved in the chips formation process during machining of difficult-to-machine materials such as NHCs core. Besides that, main influencing factors on the chips formation mechanism includes; workpiece material properties, geometry of the cutting tools especially the cutting edge design of the tool, and cutting conditions includes depth of cut, width of cut, spindle speed, feed rate, and vibration amplitude in case of ultrasonic machining. However, chips formation mechanism is more complex to understand in actual experiments under the conditions of RUM process for NHCs core material due to insufficient visual accessibility of the two most important interfaces include; cutting tool with workpiece, and cutting tool interface with chips formed. In RUM process of NHCs core material, the rapid movement of the tool especially the high ultrasonic vibration at resonant frequency of  $\geq 20$  KHz, and movement of the workpiece makes more difficult to reveal chips formation mechanism visually. Therefore, 3D FE modelling and cutting simulations technology was employed to reveal the chips formation mechanism in terms of cutting tool interface with NHCs core workpiece and

various stages of chips formation during the RUM process. Moreover, the influence of the tool geometry in terms of cutting edge design such as UCSB cutting tool under similar processing conditions of RUM was studied in order to validate the proposed 3D FE cutting simulation model of NHCs core material. In composite materials, the size and shape of the chips can be controlled by the processing conditions and fibres orientations. But in case of NHCs core material, it is made of short Nomex fibres impregnated with phenolic resin. Therefore, the chips formation mechanism in NHCs core material is different from the other composites such as CFRPs and GFRPs. Chips formation of NHCs core during RUM process by UCSB cutting tool both FE cutting simulation and experimental are shown in Figures 14(a) and 14(b).

**Figure 14** Chips formation of NHCs core during RUM process, (a) FE cutting simulations (b) RUM experiments (see online version for colours)



As shown in Figure 14, continuous chips were produced of NHCs material in RUM process with newly developed UCSB tool under similar processing conditions; width of cut 8 mm, depth of cut 2 mm, spindle speed 3,000 rpm, feed rate 500 mm/min and amplitude of tool vibration 25  $\mu\text{m}$ . It was noticed by 3D FE cutting simulation that the local stresses in the NHCs core touches the ultimate strength quickly during RUM process. So, NHCs core was machined with negligible deformation. The processing conditions to study chips formation were selected based on the experimental results and each value of processing parameter was chosen at high surface quality and low cutting force. As shown in Figure 14, less deformation observed in chips formed with UCSB tool due to sharp pointed cutting edge of UCSB tool which allows high penetration in the workpiece. Moreover, it was found by the experimental results and 3D FE cutting simulations that the main processing defects during RUM of NHCs core include tearing

of cell walls, uncut fibers and burr. Cell wall of NHCs core causes to bent by the cutting force acting on the low stiffness cutting direction of the cell wall, and also strong plasticity of the aramid paper fibres makes more difficult to break the cell wall which results in burr damages and uncut fibres. Further, the weak support on the cell walls and poor bonding strength of phenolic resin with aramid fibres causes to produce tear defects in cutting process. Thus, chips formation of NHCs core by UCSB tool includes; initially high penetration of tool in the workpiece causes to fracture the cell walls and then high-speed rotation of the tool helps to remove the material, and finally the removed material continuously slides over the flank surface of the tool which produces some contraction and deformation. Saw blade teeth are first element of new UCSB tool which comes in contact with cell walls of NHCs core. Then with the rotation and advancement of the tool in the workpiece and by damage and friction processes results in cutting and disbanding of cell walls. At this stage, chips formation will be produced from the cell walls previously cut by the saw teeth of the tool but it remains attached to the structure of the workpiece. In proceeding phase, disbanded cells of NHCs core slides on top surface of UCSB tool till end of cutting length of the workpiece. In the chips formation process, some neighbouring walls also shows very little deformation in the workpiece due to the continuous sliding of the chips on the upper face of the tool as shown in Figure 14. Ultrasonic vibration in the cutting tool causes to develop microcracks in the workpiece surface before the tool comes in contact with cutting point which leads for the easy cutting and removal of material.

## 5 Conclusions

In this paper, optimisation of RUM processing parameters and chips formation of NHCs core workpiece were studied by 3D FE modelling and cutting simulations under the conditions of RUM process. Based on the 3D FE model, series of cutting simulations and actual experimental work of RUM process on NHCs core material, the following points were concluded:

- 1 3D FE ultrasonic machining simulations and actual cutting experiments outcomes reveals that the increase in vibration amplitude causes to decrease in cutting force. Whereas, increase in feed rate results in higher cutting force. Variations in spindle speed impacts on cutting force behaviour inversely such as increase in spindle speed causes to reduce cutting force due to high kinetic energy of tool rotation which is used to remove material more quickly.
- 2 An optimised set of processing parameters was revealed in RUM of NHCs core by 3D FE cutting simulations and verified by actual RUM experimental results at resonant frequency 22,050 Hz; spindle speed 3,000 rpm, feed rate 500 mm/min, cutting width 8 mm, cutting depth 2 mm and vibration amplitude 25  $\mu\text{m}$ .
- 3 Chips formation process of NHCs core by UCSB tool includes; high penetration of tool in the workpiece causes to fracture the cell walls, high-speed rotation of the tool helps to remove the material, and finally the removed material continuously slides over the flank surface of the tool which produces some contraction and deformation. In RUM process on NHCs core, continuous chips were produced. Moreover, saw blade teeth are the first elements of UCSB tool which comes in contact with cell

walls of NHCs core. Due to impact action caused by ultrasonic vibration amplitude of the tool, microcracks developed in the cell wall of the NHCs core before the cutting tool reaches the initial contact position with workpiece during RUM process.

## Acknowledgements

The authors gratefully acknowledge the financial support for this research from the National Natural Science Foundation of China (NSFC) (Grant No. 51761145103 and Grant No. 51875311), and Shenzhen Foundational Research Project (Subject Layout) (Grant No. JCYJ20160428181916222).

## References

- Ahmad, S., Zhang, J., Feng, P., Yu, D., Wu, Z. and Ke, M. (2020a) 'Processing technologies for Nomex honeycomb composites (NHCs): a critical review', *Composite Structures*, Vol. 250, p.112545 <https://doi.org/10.1016/j.compstruct.2020.112545>.
- Ahmad, S., Zhang, J., Feng, P., Yu, D. and Wu, Z. (2020b) 'Experimental study on rotary ultrasonic machining (RUM) characteristics of Nomex honeycomb composites (NHCs) by circular knife cutting tools', *Journal of Manufacturing Processes*, Vol. 58, pp.524–535 <https://doi.org/10.1016/j.jmapro.2020.08.023>.
- Ahmad, S., Zhang, J., Feng, P., Yu, D., Wu, Z. and Ke, M. (2019) 'Research on design and FE simulations of novel ultrasonic circular saw blade (UCSB) cutting tools for rotary ultrasonic machining of Nomex honeycomb composites', *2019 16th International Bhurban Conference on Applied Sciences and Technology (IBCAST)* <https://doi.org/10.1109/IBCAST.2019.8667182>.
- Aminanda, Y., Castanié, B., Barrau, J. and Thévenet, P. (2009) 'Experimental and numerical study of compression after impact of sandwich structures with metallic skins', *Semantic Scholar* <https://doi.org/10.1016/J.COMPSCITECH.2007.10.045>.
- An, Q., Dang, J., Ming, W., Qiu, K. and Chen, M. (2019) 'Experimental and numerical studies on defect characteristics during milling of aluminum honeycomb core', *Journal of Manufacturing Science and Engineering*, Vol. 141, No. 3 <https://doi.org/10.1115/1.4041834>.
- Asmael, M., Safaei, B., Zeeshan, Q., Zargar, O. and Nuhu, A.A. (2021) 'Ultrasonic machining of carbon fiber-reinforced plastic composites: a review', *The International Journal of Advanced Manufacturing Technology*, Vol. 113, Nos. 11–12, pp.3079–3120 <https://doi.org/10.1007/s00170-021-06722-2>.
- Audibert, C., Andréani, A-S., Lainé, É. and Grandidier, J-C. (2019) 'Discrete modelling of low-velocity impact on Nomex® honeycomb sandwich structures with CFRP skins', *Composite Structures*, Vol. 207, pp.108–118 <https://doi.org/10.1016/j.compstruct.2018.09.047>.
- Baraheni, M., Tabatabaieian, A., Amini, S. and Ghasemi, A.R. (2019) 'Parametric analysis of delamination in GFRP composite profiles by performing rotary ultrasonic drilling approach: experimental and statistical study', *Composites Part B: Engineering*, Vol. 172, pp.612–620 <https://doi.org/10.1016/j.compositesb.2019.05.057>.
- Buitrago, B.L., Santiuste, C., Sánchez-Sáez, S., Barbero, E. and Navarro, C. (2010) 'Modelling of composite sandwich structures with honeycomb core subjected to high-velocity impact', *Composite Structures*, Vol. 92, No. 9, pp.2090–2096 <https://doi.org/10.1016/j.compstruct.2009.10.013>.
- Caggiano, A. (2018) 'Machining of fibre reinforced plastic composite materials', *Materials*, Vol. 11, No. 3, p.442 <https://doi.org/10.3390/ma11030442>.

- Cao, W., Zha, J. and Chen, Y. (2020) 'Cutting force prediction and experiment verification of paper honeycomb materials by ultrasonic vibration-assisted machining', *Applied Sciences*, Vol. 10, No. 13, p.4676 <https://doi.org/10.3390/app10134676>.
- Dai, G. and Mishnaevsky, L. (2014) 'Fatigue of multiscale composites with secondary nanoplatelet reinforcement: 3D computational analysis', *Composites Science and Technology*, Vol. 91, pp.71–81 <https://doi.org/10.1016/j.compscitech.2013.11.024>.
- Feng, P., Wang, J., Zhang, J. and Zheng, J. (2017) 'Drilling induced tearing defects in rotary ultrasonic machining of C/SiC composites', *Ceramics International*, Vol. 43, No. 1, pp.791–799 <https://doi.org/10.1016/j.ceramint.2016.10.010>.
- Gawryluk, J. and Teter, A. (2021) 'Experimental-numerical studies on the first-ply failure analysis of real, thin walled laminated angle columns subjected to uniform shortening', *Composite Structures*, Vol. 269, p.114046 <https://doi.org/10.1016/j.compstruct.2021.114046>.
- Giglio, M., Manes, A. and Gilioli, A. (2012) 'Investigations on sandwich core properties through an experimental-numerical approach', *Composites Part B: Engineering*, Vol. 43, No. 2, pp.361–374 <https://doi.org/10.1016/j.compositesb.2011.08.016>.
- Huang, X. (2015) 'Research on ultrasonic cutting mechanism of Nomex honeycomb composites based on fracture mechanics', *Journal of Mechanical Engineering*, Vol. 51, No. 23, p.205 <https://doi.org/10.3901/jme.2015.23.205>.
- Ivañez, I. and Sanchez-Saez, S. (2013) 'Numerical modelling of the low-velocity impact response of composite sandwich beams with honeycomb core', *Composite Structures*, Vol. 106, pp.716–723 <https://doi.org/10.1016/j.compstruct.2013.07.025>.
- Jaafar, M., Atlati, S., Makich, H., Nouari, M., Moufki, A. and Julliere, B. (2017) 'A 3D FE modeling of machining process of Nomex® honeycomb core: influence of the cell structure behaviour and specific tool geometry', *Procedia CIRP*, Vol. 58, pp.505–510 <https://doi.org/10.1016/j.procir.2017.03.255>.
- Jaafar, M., Nouari, M., Makich, H. and Moufki, A. (2021) '3D numerical modeling and experimental validation of machining Nomex® honeycomb materials', *The International Journal of Advanced Manufacturing Technology*, Vol. 115, Nos. 9–10, pp.2853–2872 <https://doi.org/10.1007/s00170-021-07336-4>.
- Kang, D., Zou, P., Wu, H., Duan, J. and Wang, W. (2019) 'Study on ultrasonic vibration-assisted cutting of Nomex honeycomb cores', *The International Journal of Advanced Manufacturing Technology*, Vol. 104, Nos. 1–4, pp.979–992 <https://doi.org/10.1007/s00170-019-03883-z>.
- Ke, M., Jianfu, Z., Pingfa, F., Zhijun, W., Dingwen, Y. and Ahmad, S. (2019) 'Design and implementation of a mini ultrasonic cutting system for Nomex honeycomb composites', *2019 16th International Bhurban Conference on Applied Sciences and Technology (IBCAST)* <https://doi.org/10.1109/IBCAST.2019.8667261>.
- Li, X., Ma, D., Liu, H., Tan, W., Gong, X., Zhang, C. and Li, Y. (2019) 'Assessment of failure criteria and damage evolution methods for composite laminates under low-velocity impact', *Composite Structures*, Vol. 207, pp.727–739 <https://doi.org/10.1016/j.compstruct.2018.09.093>.
- Liu, G., Yang, J., Zhang, L., Gao, Q., Qian, L. and Zhang, R. (2022) 'Surface quality experimental study on rotary ultrasonic machining of honeycomb composites with a circular knife cutting tool', *Crystals*, Vol. 12, No. 5, p.725 <https://doi.org/10.3390/cryst12050725>.
- Liu, H., Xie, W., Sun, Y., Zhang, J. and Chen, N. (2017) 'Investigations on micro-cutting mechanism and surface quality of carbon fiber-reinforced plastic composites', *The International Journal of Advanced Manufacturing Technology*, Vol. 94, Nos. 9–12, pp.3655–3664 <https://doi.org/10.1007/s00170-017-1110-7>.
- Liu, L., Meng, P., Wang, H. and Guan, Z. (2015) 'The flatwise compressive properties of Nomex honeycomb core with debonding imperfections in the double cell wall', *Composites Part B: Engineering*, Vol. 76, pp.122–132 <https://doi.org/10.1016/j.compositesb.2015.02.017>.

- Pascoe, J.A., Alderliesten, R.C. and Benedictus, R. (2013) 'Methods for the prediction of fatigue delamination growth in composites and adhesive bonds – a critical review', *Engineering Fracture Mechanics*, Vols. 112–113, pp.72–96 <https://doi.org/10.1016/j.engfracmech.2013.10.003>.
- Peng, B., Bergs, T., Klocke, F. and Döbbeler, B. (2019) 'An advanced FE-modeling approach to improve the prediction in machining difficult-to-cut material', *The International Journal of Advanced Manufacturing Technology*, Vol. 103, Nos. 5–8, pp.2183–2196 <https://doi.org/10.1007/s00170-019-03456-0>.
- Quino, G., Tagarielli, V.L. and Petrinic, N. (2020) 'Effects of water absorption on the mechanical properties of GFRPs', *Composites Science and Technology*, Vol. 199, p.108316 <https://doi.org/10.1016/j.compscitech.2020.108316>.
- Razanica, S., Malakizadi, A., Larsson, R., Cedergren, S. and Josefson, B.L. (2020) 'FE modeling and simulation of machining alloy 718 based on ductile continuum damage', *International Journal of Mechanical Sciences*, Vol. 171, p.105375 <https://doi.org/10.1016/j.ijmeosci.2019.105375>.
- Roy, R., Nguyen, K.H., Park, Y.B., Kweon, J.H. and Choi, J.H. (2014) 'Testing and modeling of Nomex™ honeycomb sandwich panels with bolt insert', *Composites Part B: Engineering*, Vol. 56, pp.762–769 <https://doi.org/10.1016/j.compositesb.2013.09.006>.
- Singh, R.P. and Singhal, S. (2017) 'Investigation of machining characteristics in rotary ultrasonic machining of alumina ceramic', *Materials and Manufacturing Processes*, Vol. 32, No. 3, pp.309–326 <https://doi.org/10.1080/10426914.2016.1176190>.
- Singh, R.P. and Singhal, S. (2018a) 'Experimental study on rotary ultrasonic machining of alumina ceramic: microstructure analysis and multi-response optimization', *Proceedings of the Institution of Mechanical Engineers, Part L: Journal of Materials: Design and Applications*, Vol. 232, No. 12, pp.967–986 <https://doi.org/10.1177/1464420716657370>.
- Singh, R.P. and Singhal, S. (2018b) 'Experimental investigation of machining characteristics in rotary ultrasonic machining of quartz ceramic', *Proceedings of the Institution of Mechanical Engineers, Part L: Journal of Materials: Design and Applications*, Vol. 232, No. 10, pp.870–889 <https://doi.org/10.1177/1464420716653422>.
- Singh, R.P. and Singhal, S. (2018c) 'Experimental study on rotary ultrasonic machining of alumina ceramic: microstructure analysis and multi-response optimization', *Proceedings of the Institution of Mechanical Engineers, Part L: Journal of Materials: Design and Applications*, Vol. 232, No. 12, pp.967–986 <https://doi.org/10.1177/1464420716657370>.
- Singh, R.P. and Singhal, S. (2018d) 'Experimental investigation of machining characteristics in rotary ultrasonic machining of quartz ceramic', *Proceedings of the Institution of Mechanical Engineers, Part L: Journal of Materials: Design and Applications*, Vol. 232, No. 10, pp.870–889 <https://doi.org/10.1177/1464420716653422>.
- Sun, J., Dong, Z., Wang, X., Wang, Y., Qin, Y. and Kang, R. (2020) 'Simulation and experimental study of ultrasonic cutting for aluminum honeycomb by disc cutter', *Ultrasonics*, Vol. 103, p.106102 <https://doi.org/10.1016/j.ultras.2020.106102>.
- Teng, X., Chen, W., Huo, D., Shyha, I. and Lin, C. (2018) 'Comparison of cutting mechanism when machining micro and nano-particles reinforced SiC/Al metal matrix composites', *Composite Structures*, Vol. 203, pp.636–647 <https://doi.org/10.1016/j.compstruct.2018.07.076>.
- Wang, B., Liu, Z., Song, Q., Wan, Y. and Ren, X. (2018) 'A modified Johnson-Cook constitutive model and its application to high speed machining of 7050-T7451 aluminum alloy', *Journal of Manufacturing Science and Engineering*, Vol. 141, No. 1 <https://doi.org/10.1115/1.4041915>.
- Wang, G-D. and Melly, S.K. (2017) 'Three-dimensional finite element modeling of drilling CFRP composites using ABAQUS/CAE: a review', *The International Journal of Advanced Manufacturing Technology*, Vol. 94, Nos. 1–4, pp.599–614 <https://doi.org/10.1007/s00170-017-0754-7>.

- Wang, H., Ning, F., Li, Y., Hu, Y. and Cong, W. (2019a) 'Scratching-induced surface characteristics and material removal mechanisms in rotary ultrasonic surface machining of CFRP', *Ultrasonics*, Vol. 97, pp.19–28 <https://doi.org/10.1016/j.ultras.2019.04.004>.
- Wang, H., Hu, Y., Cong, W. and Burks, A.R. (2019b) 'Rotary ultrasonic machining of carbon fiber-reinforced plastic composites: effects of ultrasonic frequency', *The International Journal of Advanced Manufacturing Technology*, Vol. 104, pp.3759–3772 <https://doi.org/10.1007/s00170-019-04084-4>.
- Wang, X., Wang, F., Gu, T., Jia, Z. and Shi, Y. (2021) 'Computational simulation of the damage response for machining long fibre reinforced plastic (LFRP) composite parts: a review', *Composites Part A: Applied Science and Manufacturing*, Vol. 143, p.106296 <https://doi.org/10.1016/j.compositesa.2021.106296>.
- Xia, Y., Zhang, J., Wu, Z., Feng, P. and Yu, D. (2019) 'Study on the design of cutting disc in ultrasonic-assisted machining of honeycomb composites', *IOP Conference Series: Materials Science and Engineering*, Vol. 611, No. 1, p.12032 <https://doi.org/10.1088/1757-899x/611/1/012032>.
- Xiang, D., Wu, B., Yao, Y., Liu, Z. and Feng, H. (2018) 'Ultrasonic longitudinal-torsional vibration-assisted cutting of Nomex® honeycomb-core composites', *The International Journal of Advanced Manufacturing Technology*, Vol. 100, Nos. 5–8, pp.1521–1530 <https://doi.org/10.1007/s00170-018-2810-3>.
- Xiong, X., Shen, S.Z., Hua, L., Liu, J.Z., Li, X., Wan, X. and Miao, M. (2018) 'Finite element models of natural fibers and their composites: a review', *Journal of Reinforced Plastics and Composites*, Vol. 37, No. 9, pp.617–635 <https://doi.org/10.1177/0731684418755552>.
- Xu, Y., Gao, Y., Wu, C., Fang, J., Sun, G., Steven, G.P. and Li, Q. (2021) 'On design of carbon fiber reinforced plastic (CFRP) laminated structure with different failure criteria', *International Journal of Mechanical Sciences*, Vol. 196, p.106251 <https://doi.org/10.1016/j.ijmecsci.2020.106251>.
- Yakun, Y., Zheng, K., Song, D., Lianjun, S. and Zhenwen, S. (2023) 'Investigation into temperature and its effects on hole wall quality in rotary ultrasonic countersinking of thin-walled CFRP/Al stacks', *Journal of Advanced Manufacturing Science and Technology*, DOI: 10.51393/j.jamst.2023002.
- Yu, H., Hu, X., Kong, L. and Yu, B. (2019) 'Process path planning based on efficiency model for ultrasonic cutting curved surface of honeycomb composite parts', *Advances in Mechanical Engineering*, Vol. 11, No. 10, p.168781401988417 <https://doi.org/10.1177/1687814019884176>.
- Zarrouk, J-E.T. (2020) 'The influence of machining conditions on the milling operations of Nomex honeycomb structure', *PalArch's Journal of Archaeology of Egypt/Egyptology*, Vol. 17, No. 6, pp.11008–11018.
- Zarrouk, T., Salhi, J-E., Atlati, S., Nouari, M., Salhi, M. and Salhi, N. (2021) 'Study on the behavior law when milling the material of the Nomex honeycomb core', *Materials Today: Proceedings* <https://doi.org/10.1016/j.matpr.2021.02.110>.
- Zha, H., Shang, W., Xu, J., Feng, F., Kong, H., Jiang, E., Ma, Y., Xu, C. and Feng, P. (2022) 'Tool wear characteristics and strengthening method of the disc cutter for Nomex honeycomb composites machining with ultrasonic assistance', *Technologies*, Vol. 10, No. 6, p.132 <https://doi.org/10.3390/technologies10060132>.
- Zhu, L., Ni, C., Yang, Z. and Liu, C. (2019) 'Investigations of micro-textured surface generation mechanism and tribological properties in ultrasonic vibration-assisted milling of Ti-6Al-4V', *Precision Engineering*, Vol. 57, pp.229–243 <https://doi.org/10.1016/j.precisioneng.2019.04.010>.
- Zinno, A., Prota, A., Di Maio, E. and Bakis, C.E. (2011) 'Experimental characterization of phenolic-impregnated honeycomb sandwich structures for transportation vehicles', *Composite Structures*, Vol. 93, No. 11, pp.2910–2924 <https://doi.org/10.1016/j.compstruct.2011.05.012>.